J|A|C|S ARTICLES

Published on Web 08/30/2010

Resolving the Au-Adatom-Alkanethiolate Bonding Site on Au(111) with Domain Boundary Imaging Using High-Resolution Scanning Tunneling Microscopy

Fangsen Li,[†,‡] Lin Tang,[‡] Wancheng Zhou,[†] and Quanmin Guo*[,‡]

State Key Laboratory of Solidification Processing, Northwestern Polytechnical University, Xi'an 710072, China, and School of Physics and Astronomy, University of Birmingham, Birmingham B15 2TT, U.K.

Received June 28, 2010; E-mail: Q.Guo@bham.ac.uk

Abstract: The bonding sites for Au-adatom-octanethiolate within the $(\sqrt{3}\times\sqrt{3})$R30° structure on Au(111) have been investigated with high-resolution scanning tunneling microscopy (STM) imaging. By establishing the relationship between the lateral positions of adsorbates on the top layer of gold and those inside an etch pit, we are able to determine the adsorption configuration with a high degree of accuracy for the elusive $(\sqrt{3}\times\sqrt{3})$R30° molecular layer. The boundary between adjacent SAM domains is also imaged with molecular resolution that allows the assignment of adsorption site in each domain without ambiguity. The standard $(\sqrt{3}\times\sqrt{3})$R30° alkanethiol SAM on Au(111) is found to consist of domains with Au-adatom-octanethiolate occupying the fcc hollows site, alongside domains where the hcp hollow site is occupied.

Introduction

Self-assembled monolayers (SAMs) of molecules have been studied extensively for over 20 years due to their interesting physical properties and potential applications.[1−5] Among the many types of SAMs, alkanethiol monolayer on the Au(111) surface is the most thoroughly investigated system[6−26] and yet the surface structure of this type of SAMs has not been fully resolved.[27,28] Even for the highly ordered, and seemingly simple $(\sqrt{3}\times\sqrt{3})$R30°, phase, the exact adsorbate bonding site and the nature of the adsorbate itself are still under debate.[29,30] Early studies assumed direct bonding between the S headgroup of $[CH_3(CH_2)_nS-]$ and surface gold atoms on unreconstructed Au(111), with all the possible high symmetry bonding sites considered: fcc hollow, hcp hollow, bridge, and atop site. The agreement between different studies, however, is rather poor. A recent investigation[29] has identified that $[CH_3(CH_2)_nS-]$ is bonded to a gold adatom to form a Au-adatom-thiolate, $[CH_3(CH_2)_nS-Au]$, and the $(\sqrt{3}\times\sqrt{3})$R30° phase is considered to consist of 0.33 monolayer (ML) of $[CH_3(CH_2)_nS-Au]$ on top of Au(111)-(1×1). The presence of gold adatoms within

[†] Northwestern Polytechnical University.
[‡] University of Birmingham.

(1) Ulman, A. *An Introduction to Ultrathin Organic Films: from Langmuir-Blodgett to Self-assembly*; Academic Press: San Diego, CA, 1991.
(2) Castner, D. G.; Ratner, B. D. *Frontiers in Surfaces Science and Interface Science*; Duke, C. B., Plummer, E. W., Eds.; North Holland: Amsterdam, 2002; p 28.
(3) Love, J. C.; Estroff, L. A.; Kriebel, J. K.; Nuzzo, R. G.; Whitesides, G. M. *Chem. Rev.* **2005**, *105*, 1103.
(4) Schreiber, F. *J. Phys.: Condens. Matter* **2004**, *16*, R881.
(5) Vericat, C.; Vela, M. E.; Benitez, G. A.; Martin Gago, J. A.; Torrellels, X.; Salvarezza, R. C. *J. Phys: Condens. Matter* **2006**, *18*, R867.
(6) Poirier, G. E. *Langmuir* **1999**, *15*, 1167.
(7) Poirier, G. E.; Pylant, E. D. *Science* **1996**, *272*, 1145.
(8) (a) Maksymovych, P.; Sorescu, D. C.; Yates, J. T., Jr. *Phys. Rev. Lett.* **2006**, *97*, 146103. (b) Maksymovych, P.; Sorescu, D. C.; Jordan, K. D.; Yates, J. T., Jr. *Science* **2008**, *322*, 1664. (c) Voznyy, O.; Dubowski, J. J.; Yates, J. T.; Maksymovych, P. *J. Am. Chem. Soc.* **2009**, *131*, 12989.
(9) Toerker, M.; Staub, R.; Fritz, T.; Schmitz-Hubsch, T.; Sellam, F.; Leo, K. *Surf. Sci.* **2000**, *445*, 100.
(10) Sharma, M.; Komiyama, M.; Engstrom, J. R. *Langmuir* **2008**, *24*, 9937.
(11) Lussem, B.; Muller-Meskamp, L.; Karthauser, S.; Waser, R. *Langmuir* **2005**, *21*, 5256.
(12) Arce, F. T.; Vela, M. E.; Salvarezza, R. C.; Arvia, A. J. *J. Chem. Phys.* **1998**, *109*, 5703.
(13) Xiao, X.; Wang, B.; Zhang, C.; Yang, Z.; Loy, M. M. T. *Surf. Sci.* **2001**, *472*, 41.
(14) Guo, Q.; Sun, X.; Palmer, R. E. *Phys. Rev. B* **2005**, *71*, 035406.
(15) Keel, J. M.; Yin, J.; Guo, Q.; Palmer, R. E. *J. Chem. Phys.* **2002**, *116*, 7151.
(16) Dubois, L. H.; Zegarski, B. R.; Nuzzo, R. J. *J. Chem. Phys.* **1993**, *98*, 678.
(17) Camillone, N., III; Eissenberger, P.; Leung, T. Y. B.; Schwartz, P.; Scoles, G.; Poirier, G. E.; Tarlov, M. J. *J. Chem. Phys.* **1994**, *101*, 11031.
(18) Pflaum, J.; Bracco, G.; Schreiber, F.; Colorado, R., Jr; Shmakova, O. E.; Lee, T. R.; Scoles, G.; Kahn, A. *Surf. Sci.* **2002**, *498*, 89.
(19) Ishida, T.; Hara, M.; Kojima, I.; Tsuneda, S.; Nishida, N.; Sasabe, H.; Knoll, W. *Langmuir* **1998**, *14*, 2092.
(20) Noh, J.; Kato, H.; Kawai, M.; Hara, M. *J. Phys. Chem. B* **2006**, *110*, 2793.
(21) Torrelles, X.; Barrena, E.; Munuera, C.; Rius, J.; Ferrer, S.; Ocal, C. *Langmuir* **2004**, *20*, 9396.
(22) Fenter, P.; Eisenberger, P.; Liang, K. S. *Phys. Rev. Lett.* **1993**, *70*, 2447.
(23) Roper, M. G.; Skegg, M. P.; Fisher, C. J.; Lee, J. J.; Dhanak, V. R.; Woodruff, D. P.; Jones, R. G. *Chem. Phys. Lett.* **2004**, *389*, 87.
(24) Picraux, L. B.; Zangmeister, C. D.; Batteas, J. D. *Langmuir* **2006**, *22*, 174.
(25) Chailapakul, O.; Sun, L.; Xu, C. J.; Crooks, R. M. *J. Am. Chem. Soc.* **1993**, *115*, 12459.
(26) Nishida, N.; Hara, M.; Sasabe, H.; Knoll, W. *Jpn. J. Appl. Phys.* **1997**, *36*, 2379.
(27) Chaudhuri, A.; Jackson, D. C.; Lerotholi, T. J.; Jones, R. G.; Lee, T.-L.; Detlefs, B.; Woodruff, D. P. *Phys. Chem. Chem. Phys.* **2010**, *12*, 3229.
(28) Li, F.; Tang, L.; Zhou, W.-C.; Guo, Q. *Langmuir* **2010**, *26*, 9484.
(29) Yu, M.; Bovet, N.; Satterley, C. J.; Bengio, S.; Lovelock, K. R. J.; Milligan, P. K.; Jones, R. G.; Woodruff, D. P.; Dhanak, V. *Phys. Rev. Lett.* **2006**, *97*, 166102.
(30) Kautz, N. A.; Kandel, S. A. *J. Am. Chem. Soc.* **2008**, *130*, 6908.

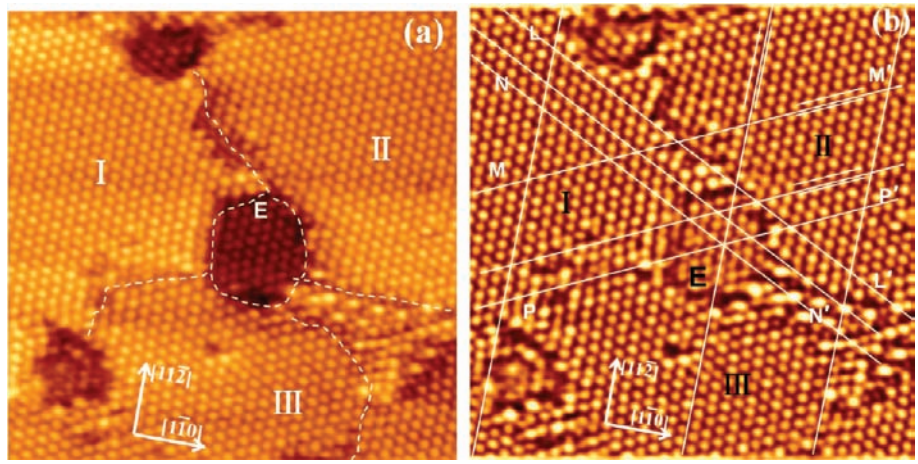

Figure 1. (a) STM image, 16.5 nm ×16.5 nm, obtained using 1.5 V sample bias and 50 pA tunnelling current from Au(111) with a saturation layer of Au-thiolate in the ($\sqrt{3}\times\sqrt{3}$)R30° phase. Dotted lines mark the domain boundaries. (b) The same image as (a) after digital filtering. White lines are drawn into the image to show the alignment of adsorbates inside the etch pit "E" with those outside, as well as the alignment between different domains.

the alkanethiol SAM has been confirmed by independent experiments although there are still discrepancies over the exact coverage of the adatoms.[31,32] A low temperature STM study has found the existence of Au-adatom-dithiolate species, $[CH_3(CH_2)_nS-Au-S(CH_2)_nCH_3]$, at low to medium coverage for relatively short-chain-length alkanethiol.[8] These experimental studies have been followed by a number of theoretical calculations[33−35] with a view to determining the most stable adsorbate structure. However, findings from various calculations have so far been inconsistent with one another and at least three rather different structural models have been proposed.[8,33,35] Here we present a high-resolution STM study of the ($\sqrt{3}\times\sqrt{3}$)R30° phase of octanethiol monolayer on Au(111). STM images from a perfectly ordered ($\sqrt{3}\times\sqrt{3}$)R30° phase do not usually contain a sufficient amount of information about the adsorption site. This is because the ($\sqrt{3}\times\sqrt{3}$)R30° phase corresponds to a saturation coverage and hence there is no bare Au(111) serving as a reference. Although a unique adsorption site always leads to a well-defined surface lattice, the reverse is not necessarily true. This is the main difficulty when one attempts to deduce the adsorption site from STM images. Here we demonstrate that we can overcome this difficulty by finding the correlation between the adsorption sites inside and outside of an etch pit, as well as that between two adjacent domains on the same atomic terrace, on Au(111) and hence using this correlation to determine the true adsorption site for Au-adatom-thiolate. Using a similar method by comparing the positional relationship between adsorbates in a striped phase, ($5\sqrt{3}\times\sqrt{3}$), and those in the ($\sqrt{3}\times\sqrt{3}$)R30° phase, we have already found that adsorbates in the ($\sqrt{3}\times\sqrt{3}$)R30° phase take either the fcc hollow or the hcp hollow site.[28] It was not known at that time exactly which type of hollow sites are occupied or whether it is possible for both types of hollow sites to be occupied on the same surface. New findings reported in the present paper provide further experimental evidence showing that, on Au(111), the ($\sqrt{3}\times\sqrt{3}$)R30° SAM consists of fcc and hcp domains. The different domains have almost the same appearance in STM images. However, a characteristic fcc−hcp translational shift can be observed between an fcc domain and its neighboring hcp domain. Within each domain, either fcc or hcp hollow site is occupied, but not both.

Experimental Section

We conducted our experiments in ultrahigh vacuum (UHV) at room temperature (RT) with a base pressure of 5×10^{-10} mbar using an Omicron VT-STM. The Au(111) sample was a thin film (~400 nm) prepared by thermal evaporation of gold onto a mica substrate in a BOC Edwards Auto 306 deposition system. The freshly prepared Au(111) sample was then transferred into a 1 mM 1-octanethiol solution in ethanol (99.5%) and left for 24 h at room temperature for the completion of the 1-octanethiol monolayer. The sample with the SAM was then taken out of the solution and thoroughly rinsed with pure ethanol and dried under N_2 flux. After the drying process, the sample was transferred to the UHV system for STM scanning without further treatment.

Results and Discussion

Figure 1a shows an STM image from Au(111) with saturation coverage of adsorbed Au-thiolate. This image has typical features of an alkanethiol SAM: close-packed adsorbates with the ($\sqrt{3}\times\sqrt{3}$)R30° structure and single-layer-deep etch pits. Before we move on to describe the detailed features of this image, we would like to make a statement and clarify what is imaged as protrusions in our STM images. In all our images the bright spots do not come out from the methyl tail groups, they are associated with the head groups at the SAM/Au interface. Under some special imaging conditions at low temperature, it has been reported that both the tail group and the headgroup can be imaged.[36] However, at RT, according to atom scattering studies, the tail groups are disordered[37] although the head groups remain to be ordered as confirmed by LEED. The reason that we do not image the methyl group is that there are no molecular levels accessible for electron transport through the hydrocarbon chain of the thiol molecule under the tunnelling conditions used in our experiment.

(31) Li, F.; Zhou, W. C.; Guo, Q. *Phys. Rev. B* **2009**, *79*, 113412.
(32) Mazzarello, R.; Cossaro, A.; Verdini, A.; Rousseau, R.; Casalis, L.; Danisman, M. F.; Floreano, L.; Scandolo, S.; Morgante, A.; Scoles, G. *Phys. Rev. Lett.* **2007**, *98*, 016102.
(33) Gronbeck, H.; Hakkinen, H.; Whetten, R. L. *J. Phys. Chem. C* **2008**, *112*, 15940.
(34) Torres, E.; Biedermann, P. U.; Blumenau, A. T. *Int. J. Quantum Chem.* **2009**, *109*, 3466.
(35) Cossaro, A.; Mazzarello, R.; Rousseau, R.; Casalis, L.; Verdini, A.; Kohlmeyer, A.; Floreano, L.; Scandolo, S.; Morgante, A.; Klein, M. L.; Scoles, G. *Science* **2008**, *321*, 943.
(36) Han, P.; Kurland, A. R.; Giodano, A. N.; Nanayakkara, S. U.; Blake, M. M.; Pochas, C. M.; Weiss, P. S. *ACS Nano* **2009**, *3*, 3115.
(37) Camillone, N.; Chidsey, C. E. D.; Liu, G. Y.; Putvinski, T. M.; Scoles, G. *J. Chem. Phys.* **1991**, *94*, 8493.

Organization of adsorbates inside the etch pits is very well resolved in the image shown in Figure 1, which allows us to determine the correlation of the lateral positioning of the adsorbates across the etch pit boundary. To establish such a correlation, the image in Figure 1a has been treated with digital filtering so that the adsorbates on different height levels are brought to the same level, Figure 1b. The image shown in Figure 1a is of good enough quality for the quantitative analysis shown below, so filtering is in fact not necessary for data analysis, but it helps the reader to identify key features more easily.

Roman numerals I, II, and III in the image denote three domains laterally shifted from one another. The pit, E, is one layer of gold lower than the atomic terrace containing domains I, II and III. Height profile across the pit can be found in the Supporting Information. In addition to the image shown in Figure 1, we have analyzed other images containing etch pits, with an example given also in the Supporting Information. Dashed lines are drawn into Figure 1a to indicate the boundaries between the domains. Lines M−M′ and P−P′ in Figure 1(b) show that the rows in domain I are offset, by 0.16 nm, relative to the rows in domain II. Lines N−N′ and P−P′ show that the rows in the pit are perfectly aligned with the rows in domain I in the two independent directions indicated. Since the overall structure has a simple 3-fold symmetry, alignment in two principal directions leads automatically to alignment in the third principal direction. Therefore, ignoring their height difference, the adsorbed species inside the pit can be described as an integral part of a two-dimensional lattice containing domain I. This perfect alignment for adsorbates on two (111) planes of different heights immediately introduces constraints as to what adsorption site the Au-thiolate should take. The (111) planes of gold are stacked with ABCABC sequence, so every third atomic plane is identical. The pit is one atomic layer deep, so its relation with the topmost layer is AB, BC, or CA. For clarity of discussion, we arbitrarily assume the top layer is A, then the layer below in the pit is shifted horizontally by $(\sqrt{3}/4)a$ in the $[11\bar{2}]$ direction where a is the nearest neighbor distance for gold atoms.

We now introduce ball models, Figure 2, to test which adsorption site is consistent with the STM image shown in Figure 1. To make the discussion clearer, we will start by assuming that the adsorbate unit is a Au-adatom-monothiolate, as proposed by Woodruff,[29] and in the process we will gradually introduce other adsorbate units and finally determine which proposed unit agrees with experimental findings. As far as STM imaging is concerned, there has been a long-standing issue as to which end of the thiol molecule gives rise to the bright contrast in the image.[36] This issue is particularly relevant to SAMs because the molecular chain is tilted by ~30° from the surface normal so the head and the tail take different (x, y) coordinates on the surface. We take the view that the bright spots in our STM images taken at room temperature correspond to the S−Au head groups. This view is based on previous atom scattering studies[37] that find the loss of positional ordering of the CH_3 groups at temperatures above 100 K while the ordering of the head groups is maintained at temperatures well above RT. At temperatures below 100 K, the ordering of the CH_3 group could be visible as reported by Han et al.[36]

For the ball models shown in Figure 2, in each case two layers of gold atoms are drawn; the upper layer represents domain I, and the lower layer represents the etch pit E. We begin by placing the Au-adatom-monothiolate on any one of the possible high symmetry sites in domain I, and then extend the two-dimensional adsorbate lattice into the pit. In Figure 2a, we arbitrarily place the Au-adatom-thiolate on the fcc hollow site on the top layer. Inside the pit, the

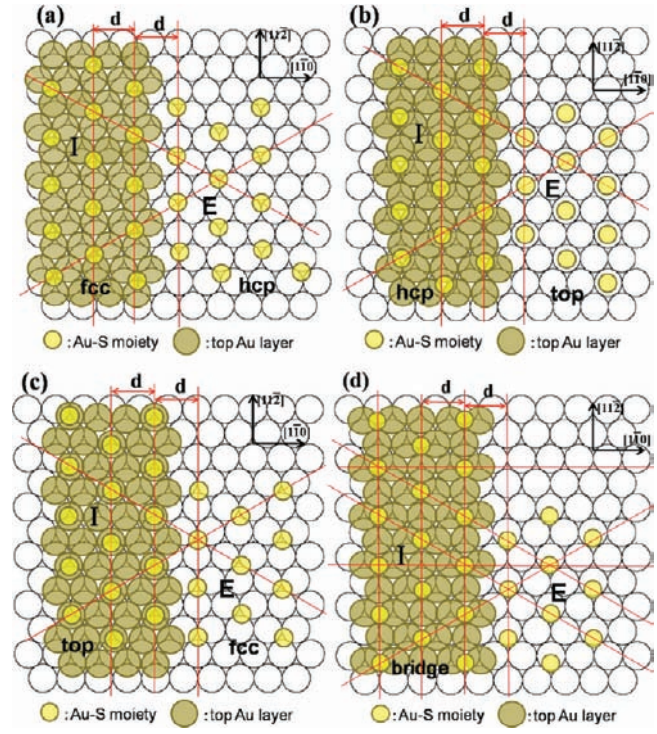

Figure 2. Ball models of possible Au-adatom-thiolate adsorption sites based on the STM image of Figure 1. Adsorption site in domain I is arbitrarily assigned to (a) fcc; (b) hcp; (c) atop; and (d) bridge.

adsorption site is chosen in such a way that the lateral positions of the thiolate species, both inside and outside the pit, map uniformly onto a single two-dimensional lattice. It is found that a perfect lateral alignment of all Au-thiolate is achieved if, and only if, the adsorption site inside the pit is the hcp hollow site. Hence, as far as lateral positioning is concerned, the model shown in Figure 2a has a 100% match with findings from the STM image. If we put the Au-adatom-thiolate on the hcp hollow site on the top layer as shown in Figure 2b, then Au-thiolate inside the pit needs to go on the atop site to maintain the experimentally observed alignment. For the same reason, if we place the Au-adatom-thiolate on the atop site over the top layer, Figure 2c, then the fcc hollow site should be occupied inside the pit. Finally, if we choose the bridge site for the Au-thiolate in domain I, it is not possible to find any high symmetry adsorption site inside the pit to maintain the lateral registry. In Figure 2d, we have tried to extend the two-dimensional overlayer lattice from domain I into the pit. By doing this, we find that the Au-thiolate species have to occupy a rather unusual low symmetry bonding site inside the pit. In the model of Figure 2d, if the Au-thiolate species were allowed to shift down in the $[\bar{1}\bar{1}2]$ direction by $(\sqrt{3})a/6$, they would occupy the high symmetry hcp hollow site. However, such a shift by $(\sqrt{3})a/6$ (0.83 Å) is not found in our STM images.

The low symmetry adsorption site shown in Figure 2d is unrealistic. Indeed, such low symmetry site has never been considered possible in previous investigations. Hence, we conclude that the bonding configuration as shown in Figure 2d is not feasible, and consequently Au-thiolate cannot stay on the bridge site in domain I. Since domain I is an arbitrary domain on the surface, we can make a conclusion that in general bridge bonding of Au-thiolate on Au(111) does not occur in the $(\sqrt{3}\times\sqrt{3})R30°$ phase. The configurations shown in Figures 2b and 2c are also ruled out for the following reasons. Each configuration involves two rather different adsorption sites: hollow (fcc or hcp) and atop. For two different adsoption sites

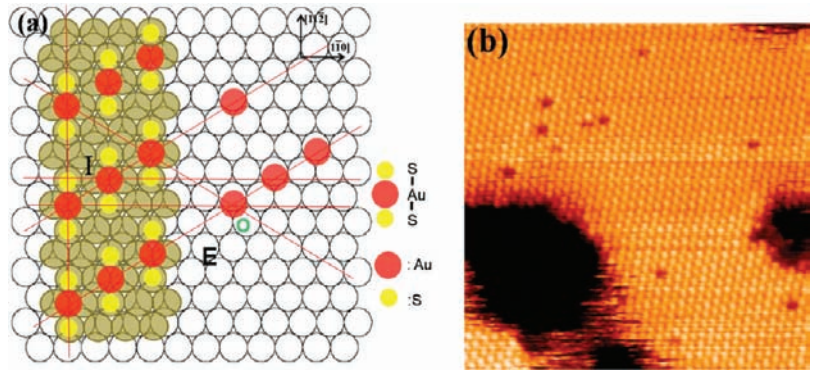

Figure 3. (a) Ball model illustrating the problem with Au-adatom-dithiolate occupying the bridge site. (b) STM image, 25 nm × 25 nm, obtained using −1.5 V sample bias and 50 pA tunnelling current, demonstrating that vacancies within the SAM are almost exclusively single-spot vacancies.

to be occupied by the Au-thiolates on the same surface at the same time, there must be little adsorption energy difference between the two sites. In an earlier study,[38] it was shown that the adsorption energy for a single gold atom, without the thiolate, on Au(111) with atop bonding is about 0.2 eV higher than that for bonding to an fcc hollow site, while the adsorption energy for the hcp site is only 0.014 eV higher. Although we are not dealing with the adsorption of isolated gold atoms here, a similarly large adsorption energy difference, ~0.2 eV, between the fcc hollow sites and the atop site is expected to exist for the Au-adatom-thiolate species. On this ground, we judge that the bonding schemes shown in Figures 2b and 2c as unrealistic even though they are consistent with the STM data. Therefore, the only possible adsorption configuration that completely agrees with experiment is the one shown in Figure 2a.

By eliminating the bridge bonded species, we have effectively also eliminated the possibility of Au-adatom-dithiolate as the basic unit in the close-packed octanethiol monolayer. The Au-adatom-dithiolate model involves the Au adatom occupying the bridge site, and according to the above analysis, a boundary is inevitable between bridge-bonded SAM inside the pit and bridge-bonded SAM on the layer above. The absence of any such boundary in the STM image suggests that the full monolayer does not contain Au-adatom-dithiolate. The Au adatom in Au-adatom-dithiolate cannot occupy sites other than the bridge site, because the S atoms must be positioned right above gold atoms in a local atop configuration.[39] Au-adatom-dithiolate has been found to exist for low coverage SAMs as shown previously for dimethyl disulfide adsorption[8] and more recently for low coverage butanethiol SAM on Au(111).[27] To assist the reader, we have included a schematic diagram, Figure 3a, to illustrate how the inclusion of Au-adatom-dithiolate species conflicts with experimental observations. In Figure 3a, on the upper terrace the dithiolate species are drawn according to the scheme proposed for methyl-dithiolate.[8] The Au adatom occupies the bridge site, and the two sulfur atoms occupy atop sites. If we translate this arrangement to the lower terrace, we immediately run into trouble because the Au adatoms on the lower terrace have to occupy low symmetry sites as illustrated in the figure. For Au-adatom-methyl-dithiolate on Au(111), it was proposed that the methyl groups appear bright in STM images. If we assume that the bright spots in our images were due to the methyl tail groups, then the number of bright spots along the $[11\bar{2}]$ direction across one domain must be always an even number because there are two hydrocarbon chains attached to a common Au adatom to form a single unit. This is contradictory to what we find that the number of bright spots along $[11\bar{2}]$ and its other two equivalent directions across a single domain can be odd or even with the same frequency of occurrence. Another evidence against the presence of Au-adatom-dithiolate is that when a vacancy is observed within the $(\sqrt{3}\times\sqrt{3})$R30° phase, it nearly always appears as one single missing spot as shown in Figure 3b rather than a pair of missing spots. Some of the vacancies are observed to diffuse within the layer, and the diffusion is also characterized by the movement of individual, rather than pairs of, dark spots. Our findings thus do not support the Au-adatom-dithiolate model for the high coverage $(\sqrt{3}\times\sqrt{3})$R30° phase. However, the existence of dithiolate species at low to medium coverages is possible, but this is not within the scope of the present study.

The above analysis is based on our understanding that the bright spots in our STM images are from the S−Au groups. Even if we assume that the spots are from the CH_3 groups, the arguments still hold as long as the molecules inside the pit tilt in the same direction as those outside. This is because the 2-D array of CH_3 groups has exactly the same structure as the array of S−Au groups for Au-adatom-monothiolate, and the two arrays are related by a simple translation operation along the direction of the tilt. If the adsorbates inside the pit tilt in a different direction than those outside, then the 2-D lattice of the CH_3 groups would not be continuous across the boundary of the etch pit and an offset between the network of CH_3 groups inside the pit and that outside would be visible. We want to point it out that this offset is dependent on both the chain length of the thiol molecule and the tilt angle, hence the chance that the offset equals exactly the unit cell dimension of the $(\sqrt{3}\times\sqrt{3})$R30° phase is extremely small considering that there is no rational relation between the chain length and the lattice constant of gold.

Next, we examine the relationship between domain I and domain II in Figure 1b. These two domains are translationally shifted to each other. Along line L−L′ in the figure, spots in the two domains are aligned, but there are no alignments in the other two close-packing directions. To quantify the translational shift, we randomly choose two spots along the line L−L′, one in each domain, and measure the distance between them. What we find is that the measured distance beween such two spots can always be expressed as $n(\sqrt{3})a + 0.16nm$. Since $(\sqrt{3})a$ is the distance between nearest neighbor spots, 0.16 nm is thus a

(38) Takeuchi, N.; Chan, C. T.; Ho, K. M. *Phys. Rev. B* **1991**, *43*, 13899.
(39) (a) Roper, M. G.; Skegg, M. P.; Fisher, C. J.; Lee, J. J.; Dhanak, V. R.; Woodruff, D. P.; Jones, R. G. *Chem. Phys. Lett.* **2004**, *389*, 87. (b) Kondoh, H.; Iwasaki, M.; Shimada, T.; Amemiya, K.; Yokoyama, T.; Ohta, T.; Shimomura, M.; Kono, S. *Phys. Rev. Lett.* **2003**, *90*, 066102.

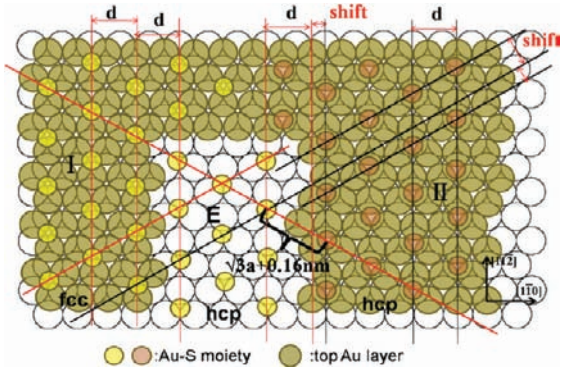

Figure 4. Relationship between two translationally shifted domains. Au-adatom-thiolate occupies the fcc hollow site in domain I, and the hcp hollow site in domain II respectively. E represents an etch pit in between the two domains.

quantitative measure of the lateral shift between the two domains. This lateral shift can be described very well by the ball model shown in Figure 4 where domain II consists of Au-adatom-thiolate sitting on hcp hollow sites. The 0.16 nm displacement correponds to an adsorption site shift from fcc hollow site to the nearest hcp hollow site, $(\sqrt{3})a/3$, at the domain boundary. As mentioned above, the adsorption energy for a gold atom on the hcp hollow site is only about 14 meV higher than that on the fcc hollow site, so the observation that both the fcc and the hcp hollow sites can be occupied at room temperature is in agreement with the small energy difference.

Figure 5a shows another example of an fcc/hcp domain boundary. In the image, there are two domains linked by a domain boundary. White lines in the image mark the positional offset between adsorbates in the domain on the left and those in the domain on the right. The domain boundary is clearly resolved so that the connection between the adsorbate postions in the two conecting domains can be accurately determined without any ambiguity. Figures 5b−e are ball models used to determine the adsorption site. The procedure here is similar to that applied to the image in Figure 1. Among the three models shown in Figure 5b−d, the one shown in Figure 5c is chosen as the most appropriate model for reasons discussed earlier. The model shown in Figure 5e, with the Au-adatom-monothiolate on bridge sites, is unable to reproduce the observed boundary structure. If the Au-adatom-monothiolate is replaced by Au-adatom-dithiolate in Figure 5e, it would produce a highly disordered domain boundary very different from the oberved structure in Figure 5a. According to the model of Figure 5c, the adsorbate rows in the two domains are offset by $d/3$, where d is the spacing between two adjacent rows in each domain. The measured offset distance from Figure 5a is 0.14 nm, which is in excellent agreement with the model. Therefore, the boundary shown in Figure 5a is formed between an fcc domain and a hcp domain.

So far we have considered only the boundary between an fcc and an hcp domain. There is also the possibility of forming a boundary between two fcc domains. This could happen if one fcc domain is shifted relative to the other by a in the $[1\bar{1}0]$ direction. It can be shown that, for two such fcc domains, there is no alignment of the Au-adatom-thiolate rows across the boundary in any of the three close-packing directions.

Conclusions

In conclusion, we have presented clear experimental evidence to show that the $(\sqrt{3}\times\sqrt{3})$R30° phase of an octanethiol monolayer consists of domains with fcc occupation by Au-adatom-monothiolate and domains of hcp occupation. Within each domain either the fcc or the hcp site is occupied. Atomically resolved domain boundary structure allows a straightforward assignment of the adsorption site without ambiguity. Although the experiment is conducted with an octanethiol monolayer, the conclusion is applicable to alkanethiol monolayers in general. Our findings help to resolve the long-standing controversy regarding the true adsorption site in alkanethiol monolayers.

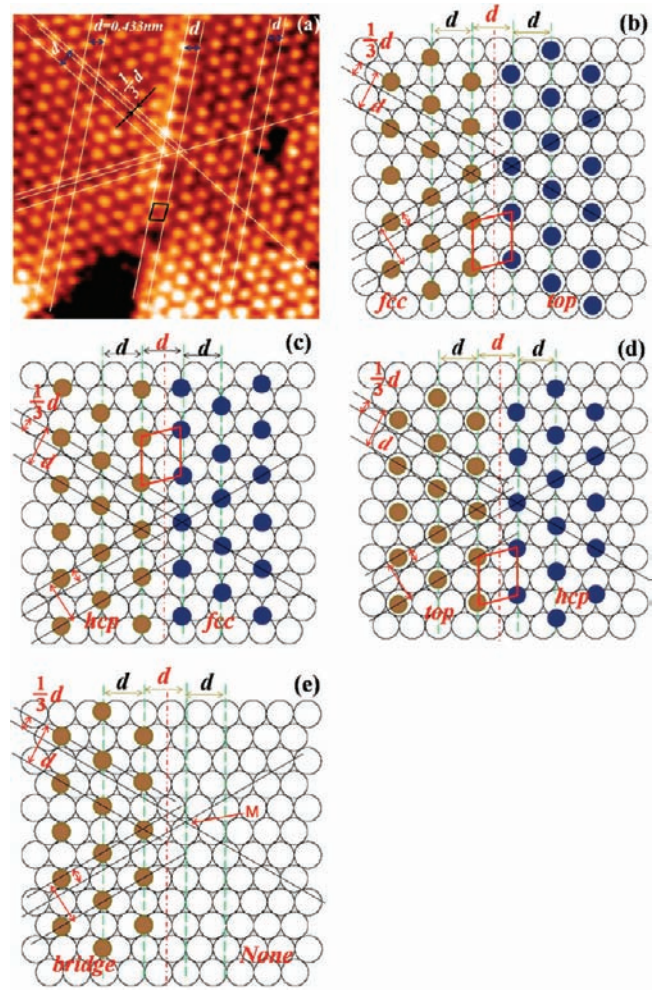

Figure 5. (a) STM image, 8.5 nm × 8.5 nm, obtained using 1.5 V sample bias and 50 pA tunnelling current, showing two $(\sqrt{3}\times\sqrt{3})$ R30° domains on the same atomic terrace. (b−e) are structural models considered using Au-adatom-monothiolate as the adsorption unit. The adsorption site in the left domain is arbitrarily assigned to (b) fcc; (c) hcp; (d) atop; and (e) bridge.

Acknowledgment. We thank the EPSRC for financial support, and F.L. thanks the Chinese Scholarship Council for providing a studentship.

Supporting Information Available: Additional figures including STM images and a height profile. This material is available free of charge via the Internet at http://pubs.acs.org.

JA1056517